In-Flight Calibration of ICA - Cross-Talk Between Azimuth Sector Anodes

Laura Berčič

IRF Technical Report 056
May 2017

ISSN 0284-1738

Institute för rymdfysik

Swedish Institute of Space Physics

Kiruna, Sweden

Swedish Institute for Space Physics

Solar System Physics and Space Technology

In-Flight Calibration of ICA

Cross-Talk Between Azimuth Sector Anodes

Author:
Laura Berčič

Supervisor:
Etienne Behar

May 24, 2017

Abstract

This paper focuses on the phenomena referred to as cross-talk, appearing between the azimuth sectors of the Ion Composition Analyzer (ICA), a part of the Rosetta Plasma Consortium. In-flight calibration was needed due to incomplete documentation of the on-ground calibration and instrument manufacture. The unidirectional beam of solar wind protons during a large part of the mission provides calibration-like conditions for most of the azimuthal coverage of the instrument. This method is thus based on scientific data. Empirically determined cross-talking sector pairs corroborate with the retrieved ICA documentation. Combining the in-flight calibration results and retrieved reports from on-ground calibration a matrix of cross-talking pairs is produced and can be applied to the full ICA data set.

Contents

1 Introduction

1.1 Instrument Overview

The Ion Composition Analyzer (ICA) is a mass spectrometer part of the Rosetta Plasma Consortium, on board the European Rosetta spacecraft. It is designed to measure the three-dimensional distribution function of positive ions in order to study the interaction between the solar wind and cometary particles in the vicinity of comet Churyumov-Gerasimenko(67P). Particles enter the instrument through a 360^o wide aperture covered with a grid, as marked on Figure 1. Behind the grid stands an electrostatic acceptance angle filter, a deflection system only accepting particles coming with a elevation angle within a range of $90°$ spanning from $-45°$ to $45°$. This angular range is covered with 16 elevation steps, giving 16 elevation bins with the width of 5^o.

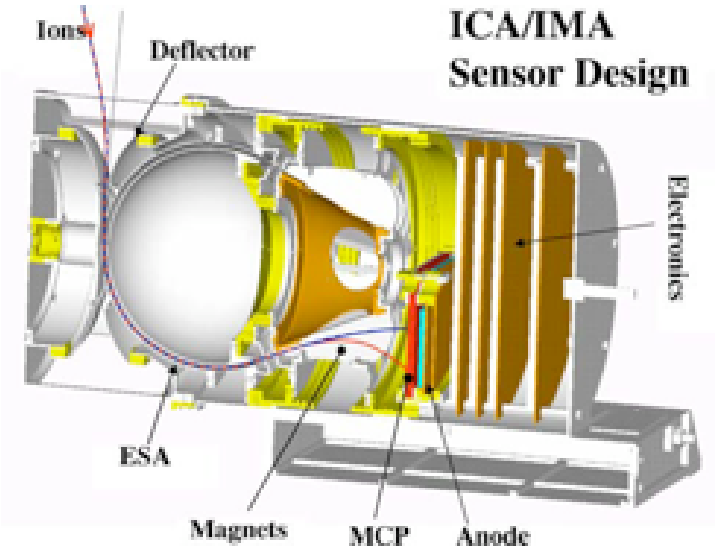

Figure 1: Cross section of the ICA sensor showing the main components of the instrument, taken from [1].

The azimuthal impact position is measured by *16 sector anodes*, giving the azimuthal resolution of 22.5^o. Sectors 10 to 15 and 0 are shadowed by the spacecraft for elevation bins from 0 to 7 (Figure 3). In the report, the field-of-view of the instrument will be presented as in Figure 4.

The in-flight calibration is needed, because the on-ground calibration made by Andrei Fedorov in CESR (Toulouse) suffered from extreme time constraints and only very little documentation is left of it. Information regarding cross-talking sectors that we were able to retrieve contains 3 colour map plots presented later on. However, some more documentation about Ion Mas Analyzer (IMA), part of Mars Express mission, is available and can be used since both ICA and IMA have the same amplifier board design.

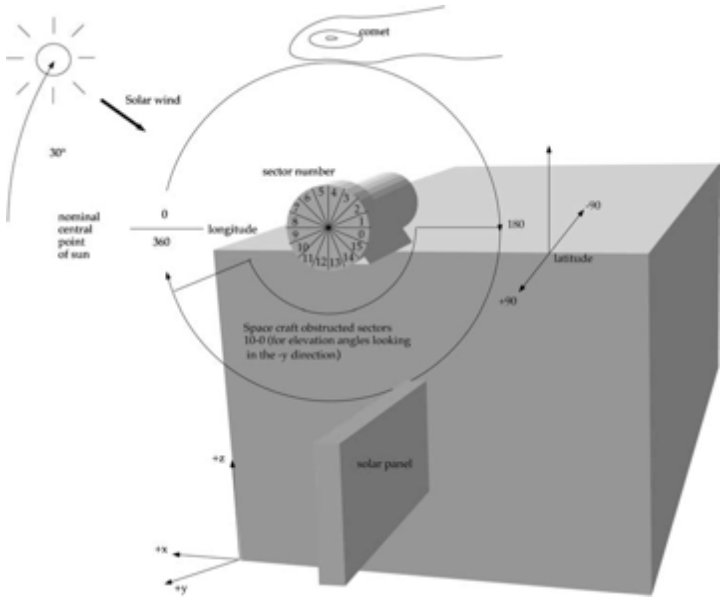

Figure 2: Schematic location of ICA on the spacecraft. Note that sector numbering in the figure corresponds to the viewing direction, not the physical location of the corresponding sector on the detector micro-channel plate (MCP), taken from [1].

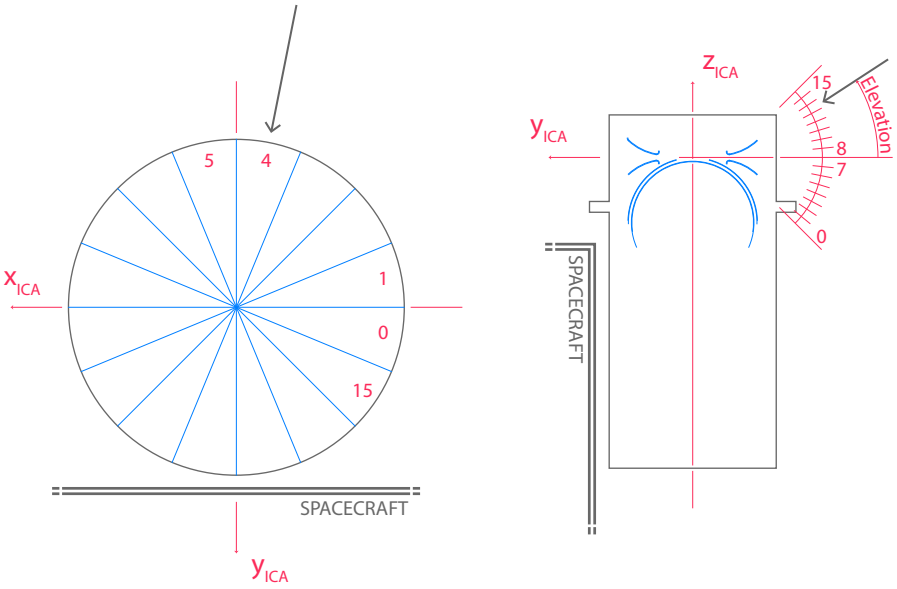

Figure 3: The numbering of the azimuth sectors and elevation bins with respect to the instrument position on the spacecraft.

1.2 About Cross-Talk

This study focuses on one precise phenomenon, referred to as electronic cross-talk. It appears that when one anode of the detection assembly is illuminated, signal also

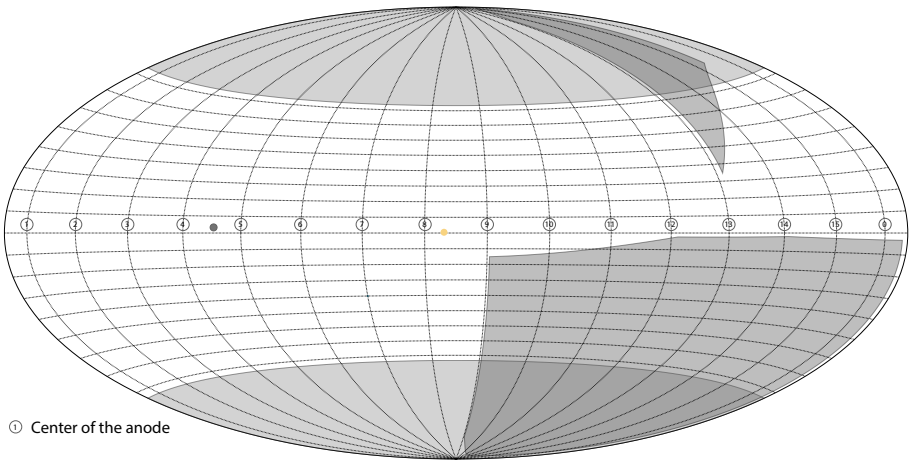

Figure 4: Empty field-of-view plot showing the sector numbering. The dark grey areas represent the shadows of the spacecraft and the solar panel. Typical positions of both the Sun (yellow dot) and the comet nucleus (grey dot) are given, as they have remained fairly static in ICA field-of-view during the entire mission.

arises from other, *unilluminated anodes*. This is likely to happen when two wires are situated too close to each other or not properly isolated, therefore transferring a part of signal from one to another. The term *emitter* is used when the signal output of the sector anode is due to the presence of particles (*e.g.* physical signal) and the term *receiver* stands for sectors that provide some signal even when no physical particle is detected. The value of cross-talk is the percentage of counts in the emitting sector that appears in the receiving sector.

The analysis is based on the expectation that the solar wind protons will enter the instrument from only one direction in a single beam. Therefore, when two signal peaks of mentioned species are observed, the weaker signal is not physical, but the effect of cross-talk phenomena. The detected proton beam is in most cases spread over at least two azimuth sectors, which prevents us to study the cross-talk between two neighbouring sectors. However, this is not a big drawback since the on-ground calibration reports show that the majority of cross-talk pairs consists of emitter and receiver positioned roughly 90^o ($\sim$4 sectors) apart.

2 Empirical Approach

2.1 Data Analysis

The scientific data used for the following analysis was collected during the active mission between September 2014 and September 2016. The Rosetta spacecraft arrived to the comet 67P at the heliocentric distance of $\sim 3.6AU$ and accompanied it along an arc of its elliptic orbit including perihelion. In the beginning of the mission, when the comet is relatively far from the Sun, nucleus activity is low and the growing cometary atmosphere is yet too thin to influence the flow of the incoming solar wind. As the comet approaches

the Sun, its atmosphere evolves, which results in an increasing deflection of the solar wind protons and eventually to a significant broadening of their velocity distribution. Furthermore, in April 2015, an expanding solar wind cavity was first observed, as the coma was growing in size and density. From April 2015, through the closest approach in September 2015 and until January 2016, when the comet is again distanced enough from the Sun, the ICA instrument was within the solar wind cavity, which explains the absence of the solar wind signal in the ICA data.

During a great part of the mission when the solar wind protons reach the instrument, they present themselves as a rather unidirectional beam. In these conditions, a high proton flux in a specific direction is expected, whereas all other smaller peaks are assumed not to be a physical measurement but electronic cross-talk. This allows us to use the solar wind protons as a narrow calibration beam. The beam normally spreads between 1 to 8 elevation steps (with the angular resolution of 5^o) and between 1 to 4 azimuth sectors (with the angular resolution of 22.5^o). Selected data sets had more than 80% of the proton counts in one azimuth sector and less than 10% of the counts in each of its neighbours and the distribution along the elevation dimension was used to compare the two sectors in a cross-talking pair.

All data sets have an equal integration time of 192 seconds during which the whole scan of 96 energy steps and 16 elevations is made. Only data with the highest angular resolution were used, which which corresponds to the operation modes 8, 16 and 24. The protons were manually selected from the daily energy mass spectra. Following figures show some examples of suitable data sets for different cross-talking pairs in the field-of-view representation, where the number of protons summed up over selected mass rings and energy bins is proportional to the size of the red dot.

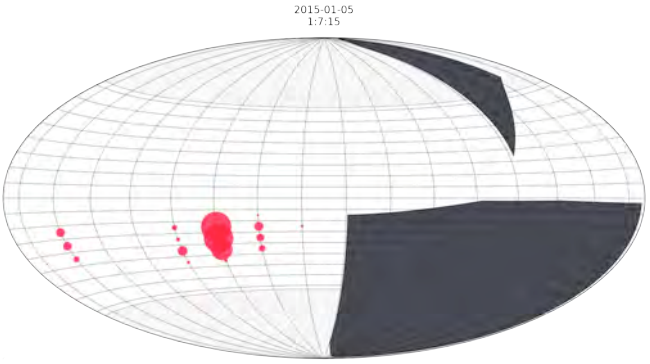

Figure 5: Physical measurement in sector 6 and cross-talk in sector 2.

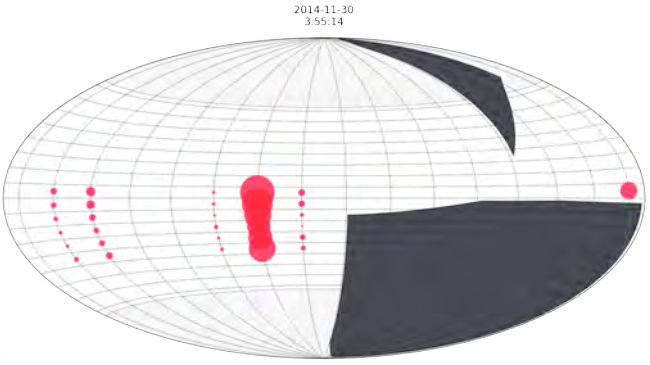

Figure 6: Physical measurement in sector 7 and cross-talk in sector 2 and 3.

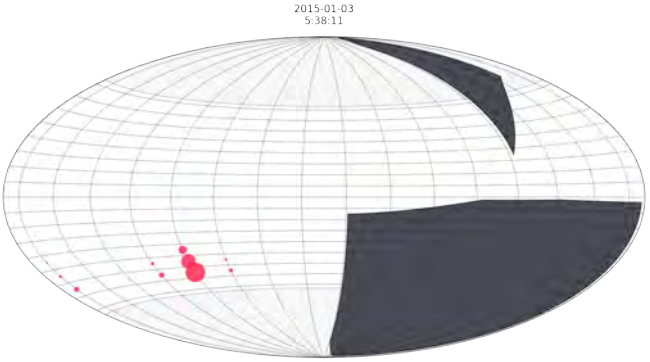

Figure 7: Physical measurement in sector 5 and cross-talk in sector 1.

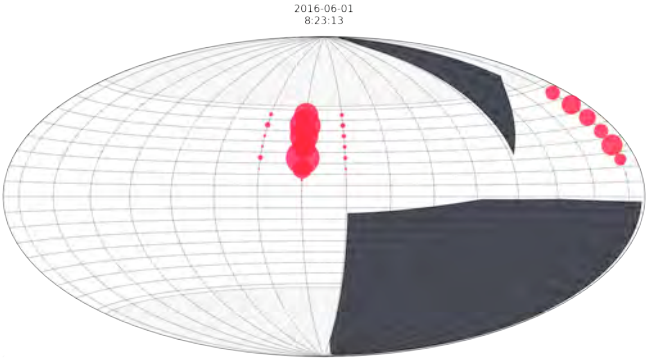

Figure 8: Physical measurement in sector 8 does not affect any other sector.

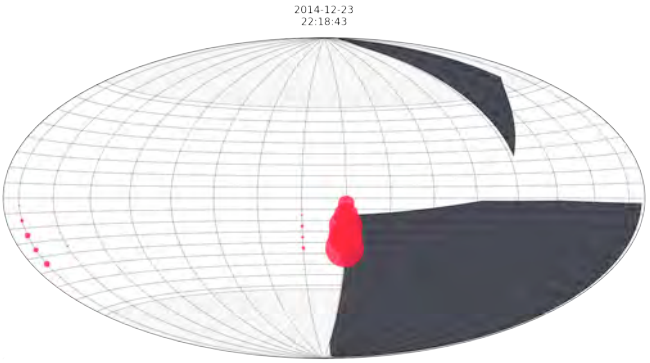

Figure 9: Physical measurement in sector 9 and cross-talk in sector 1.

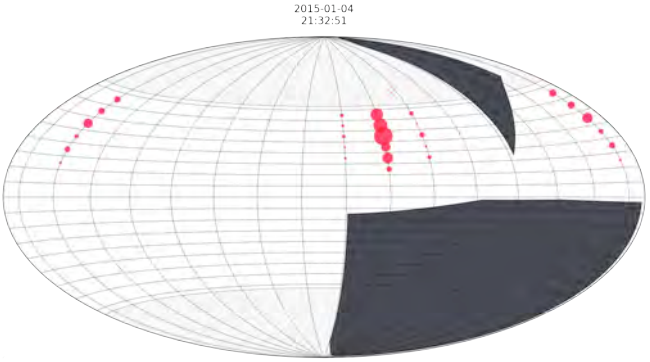

Figure 10: Physical measurement in sector 10 and cross-talk in sector 2.

Looking at the field-of-views we can easily separate between the physical signal and that of the cross-talk origin and define the cross-talking pairs. Sector 0 is treated separately, because it seems to present some value every time any of the other azimuth sectors is illuminated.

To compare emitting and receiving sector in the elevation dimension, the number of counts in each was plotted against the elevation (Figure 11 and 12). The green curve in these two plots represents the ratio between counts in receiver and emitter, what we have defined as the cross-talk value. The trend of the cross-talk curve corresponds to the other two implying that the cross-talk value varies with the number of counts in each elevation step. No other variables (like mass anode ring or elevation bin) were found to give comparably high correlation coefficients. However, it does in some cases show a small growth over time.

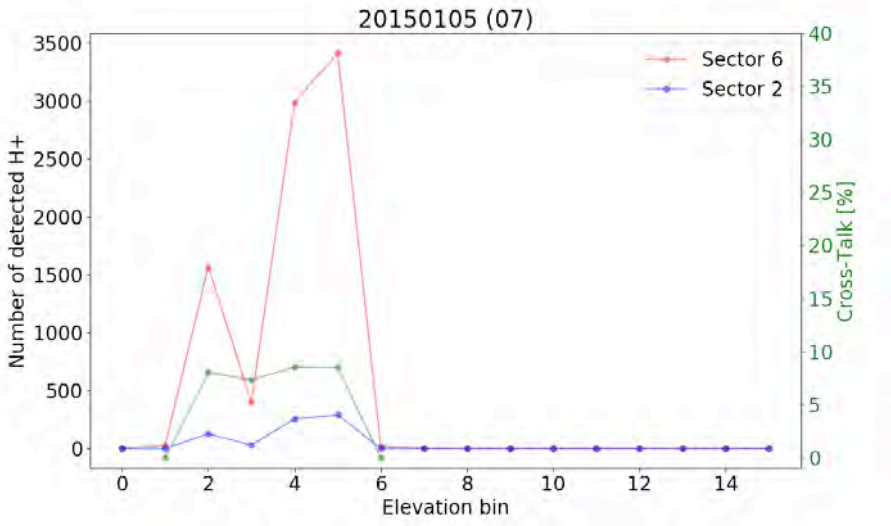

Figure 11: Comparison between sector 6 as emitter and sector 2 as receiver and the value of cross-talk between them. The counts are summed up over 192 seconds, and selected mass rings and energy bins.

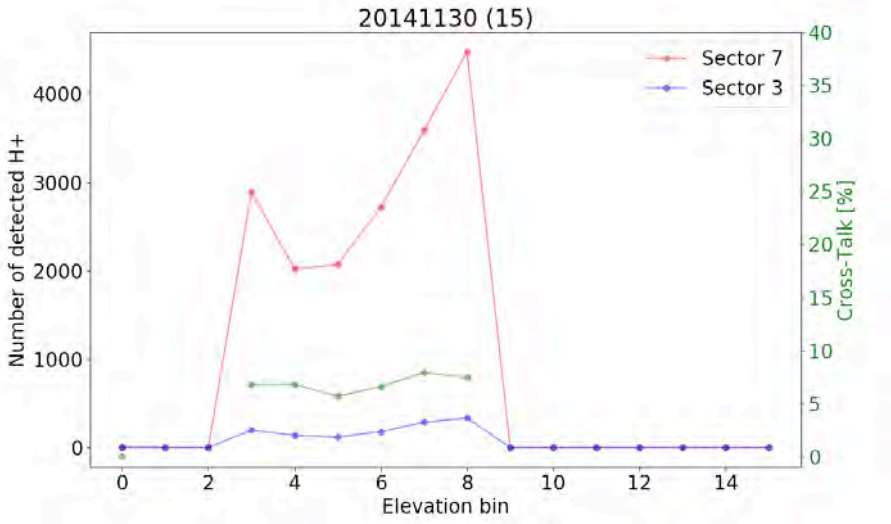

Figure 12: Comparison between sector 7 as emitter and sector 3 as receiver and the value of cross-talk between them.

2.1.1 Cross-Talking Pairs Excluding Sector 0

To further analyse the dependence between the cross-talk value and the number of detected protons, only carefully chosen data sets were considered, e.g., only highly

correlated sector pairs with most of the proton counts in a single emitting sector. Cross-talk was then calculated separately for each energy bin - elevation step pair and plotted with respect to the number of counts in this bin - step pair. The measurements exhibit a logarithmic trend, presented like

$$CT_{receiver} = [a \cdot ln(N_{emitter}) + b] \cdot N_{emitter}$$

where $N_{emitter}$ is the number of counts in emitting sector, and a and b are the function parameters noted in plots for each cross-talking pair and gathered in a Table 1.

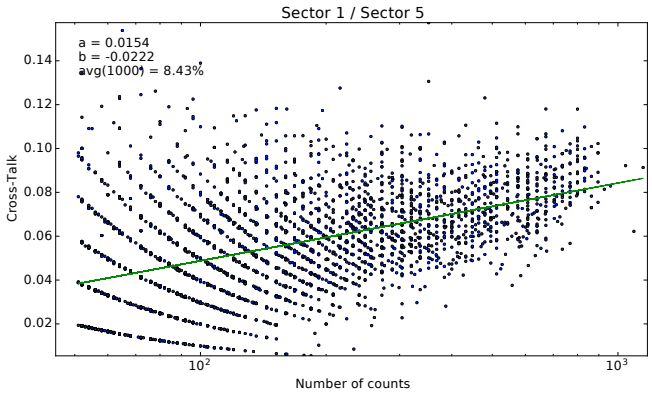

Figure 13: Cross-talk appearing in sector 1 due to sector 5.

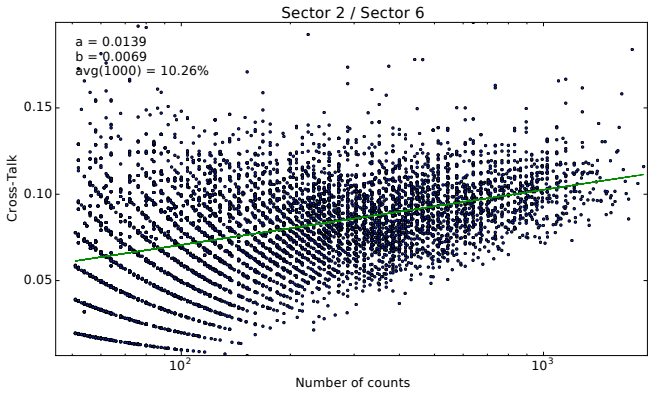

Figure 14: Cross-talk appearing in sector 2 due to sector 6.

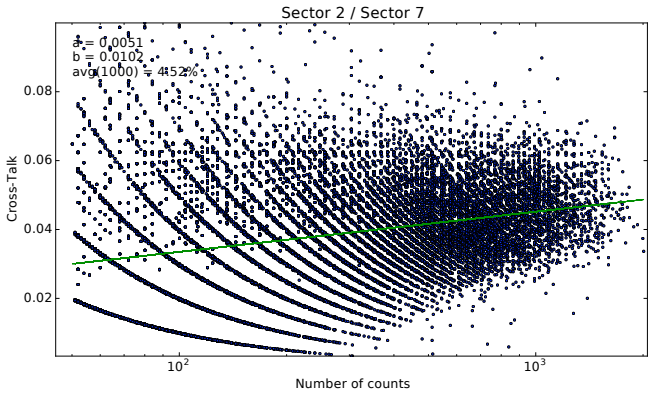

Figure 15: Cross-talk appearing in sector 2 due to sector 7.

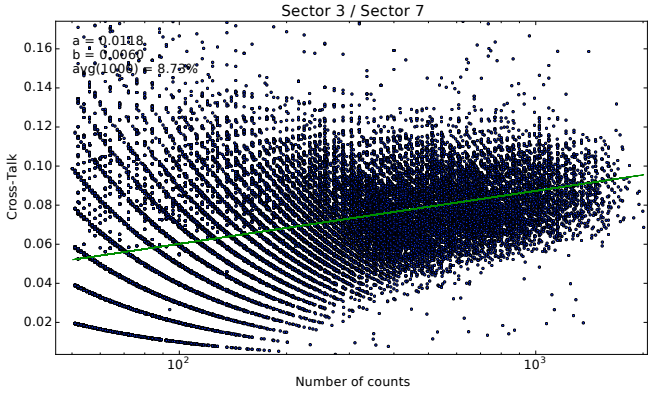

Figure 16: Cross-talk appearing in sector 3 due to sector 7.

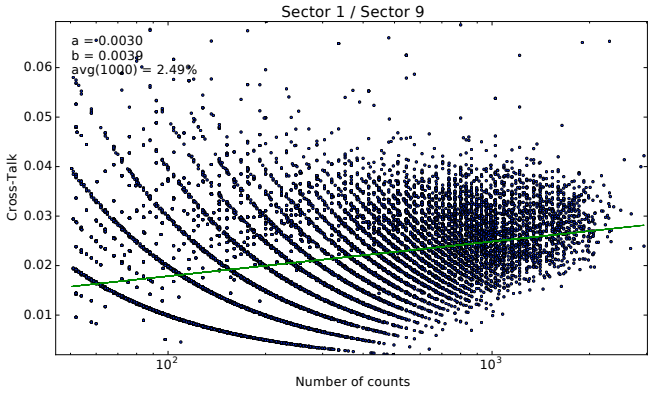

Figure 17: Cross-talk appearing in sector 1 due to sector 9.

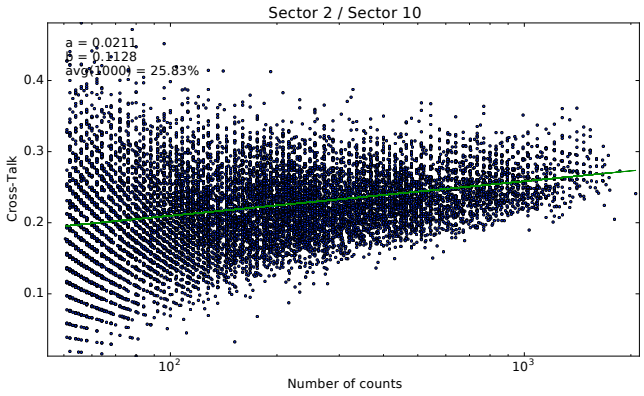

Figure 18: Cross-talk appearing in sector 2 due to sector 10.

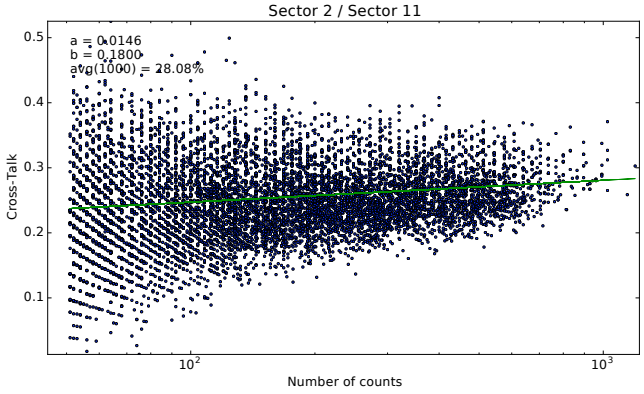

Figure 19: Cross-talk appearing in sector 2 due to sector 11.

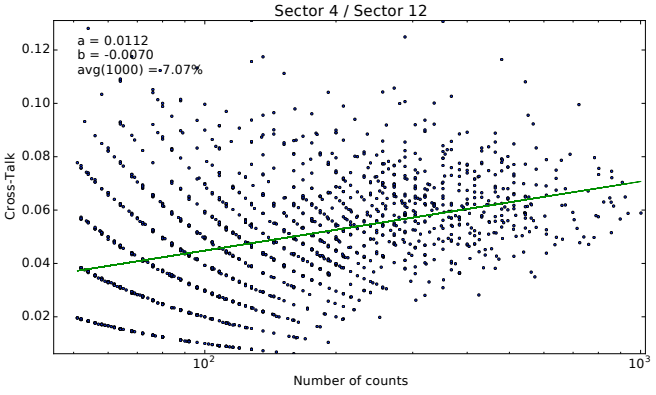

Figure 20: Cross-talk appearing in sector 4 due to sector 12.

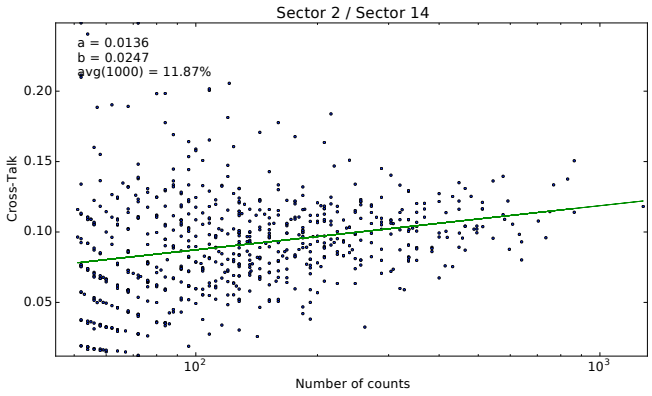

Figure 21: Cross-talk appearing in sector 2 due to sector 14.

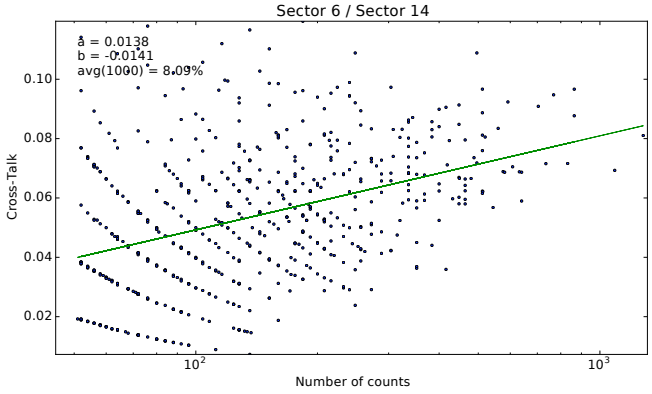

Figure 22: Cross-talk appearing in sector 6 due to sector 14.

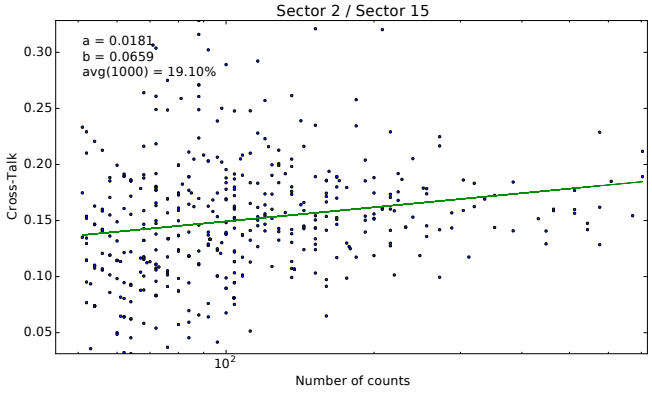

Figure 23: Cross-talk appearing in sector 2 due to sector 15.

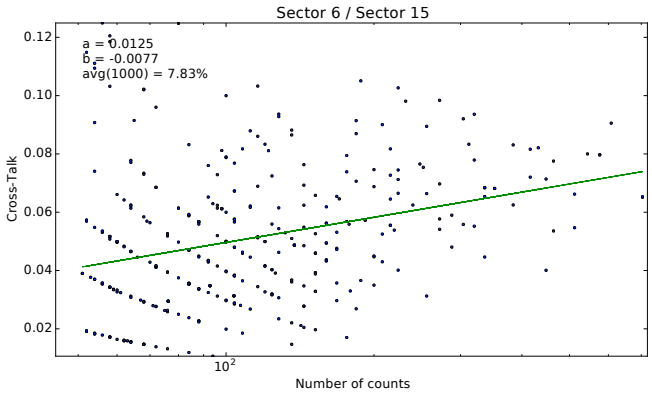

Figure 24: Cross-talk appearing in sector 6 due to sector 15.

Table 1: Table of cross-talking pairs assuming logarithmic relation between the value of cross-talk and the number of protons detected.

Emitter	Receiver	$CT_{receiver} = [a \cdot ln(N_{emitter}) + b] \cdot N_{emitter}$	
		a	b
5	1	0.0154	-0.0222
6	2	0.0139	0.0069
7	2	0.0051	0.0102
	3	0.0118	0.0060
8	/		
9	1	0.0030	0.0030
10	2	0.0211	0.1128
11	2	0.0146	0.1800
12	4	0.0112	-0.0070
14	2	0.0136	0.0247
	6	0.0138	-0.0141
15	2	0.0181	0.0659
	6	0.0125	-0.0077

2.1.2 Cross-Talk in Sector 0

Sector 0 is believed to be affected by all other sectors. Therefore the function of cross-talk accumulated in sector 0 consists of a fraction of each sector illuminated in a data set:

$$CT(0) = \sum_{\text{Emitters}} CT_{emitter}(0),$$

Usually emitter causes cross-talk on some sector other than 0 and then the receiver could contribute to the cross-talk on 0. For example, when only sector 5 is illuminated, receiving sector 1 might emit further to sector 0:

$$\begin{aligned} CT(0) &= CT_5(0) \\ &= [a_{5,0} \cdot ln(N_5) + b_{5,0}] \cdot N_5 + [a_{1,0} \cdot ln(CT_5(1)) + b_{1,0}] \cdot CT_5(1) \end{aligned}$$

$$CT_5(1) = [a_{5,1} \cdot ln(N_5) + b_{5,1}] \cdot N_5$$

Coefficients $a_{5,0}$, $b_{5,0}$, $a_{1,0}$, and $b_{1,0}$ can not be determined because, we could not be sure whether the number of counts observed in sector 0 represents cross-talk or the real physical measurement, as 1 and 0 are neighbouring sectors. However, the contribution from the first receiver to sector 0 is very small and probably within the error we make by fitting the plots in the previous section. Therefore, the results in Table 2 represent the cross-talk caused by emitters together with associated receivers.

All azimuth sectors except the dead sector 13 and the immediate neighbours of sector 0, sector 1 and 15, have been recognised as emitters to sector 0.

Table 2: Cross-talk appearing in sector 0.

Emitter	$CT_0 = [a_{emitter,0} \cdot ln(N_{emitter}) + b_{emitter,0}] \cdot N_{emitter}$	
	a	b
2	0.0145	0.2365
3	0.0144	0.2184
4	0.0122	0.2308
5	0.0198	0.0467
6	0.0116	-0.1188
7	0.0315	0.0840
8	0.0336	0.1166
9	0.0296	0.0937
10	0.0258	0.1325
11	-0.0047	0.2911
12	0.0034	0.4129
14	-0.0005	0.2211

2.1.3 Cross-Talk Over Time

As mentioned before, a small dependency of cross-talk over the whole duration of the mission was found. The first five rows in the Table 3 presenting five of the most common

and trust worthy sector pairs give similar conclusions. That is the increase of electronic cross-talk of about $\sim 11.6\%$ during the 2 years of active mission. For cross-talking pair with 6 as an emitter and 2 as a receiver the time dependence gives 1.2% per month, which for a 1000 counts in emitter changes the cross-talk in receiver for ~ 1 count. The rate is very slow and therefore not included in implementation.

Table 3: Cross-talk dependence on time for each cross-talking sector pair. Last two columns present the change of the average value over the duration of the whole active mission, 2 years.

Emitter	Receiver	$CT_{receiver} = a \cdot t\,[days] + b$		Δ over 730 days	
		$a \cdot 10^{-6}$	b	absolute	relative(%)
5	1	1.8767	0.0499	0.0137	16.3
6	2	1.9846	0.0725	0.0145	14.1
7	2	0.5891	0.0352	0.0043	9.6
	3	1.1673	0.0639	0.0085	9.8
8	/				
9	1	0.2751	0.0201	0.0020	8.0
10	2	-1.8590	0.2324	-0.0136	-5.3
11	2	-5.9497	0.2903	-0.0434	-15.4
12	4	2.7813	0.0484	0.0203	28.6
14	2	-2.3674	0.0974	-0.0173	-14.5
	6	0.5672	0.0523	0.0041	5.1
15	2	1.5651	0.1471	0.0114	6.0
	6	-0.4261	0.0528	0.0031	4.0

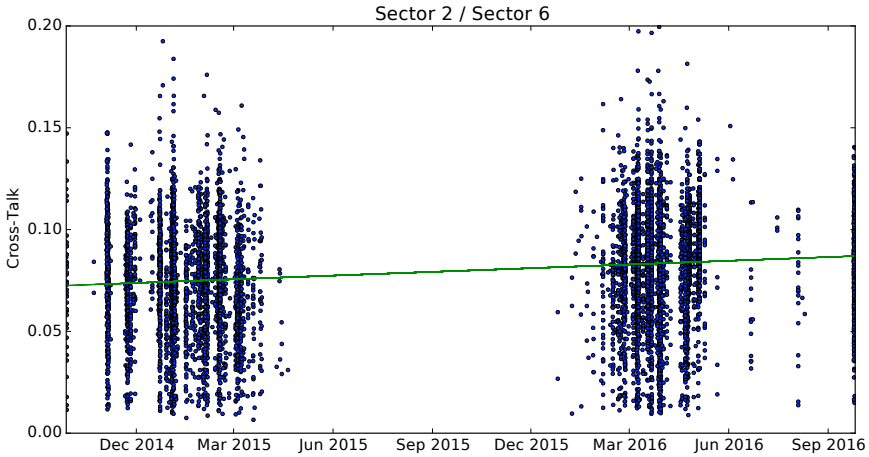

Figure 25: Example of the cross-talk over the time of the mission plot for the cross-talking pair with sector 6 as emitter and 2 as receiver.

3 Implementation

The obtained parameters are tested by subtracting the empirically predicted values of cross-talk from the data sets:

$$CT_{receiver} = \sum^{\text{CT pairs}} \left[a_{emitter,receiver} \cdot ln(N_{emitter}) + b_{emitter,receiver}\right] N_{emitter},$$

where $CT_{receiver}$ is the predicted number of counts in the receiver, $N_{emitter}$ is the number of counts in emitter, coefficients $a_{emitter,receiver}$ and $b_{emitter,receiver}$ are the ones from Table 1 and 2, and the sum is done over all cross-talking pairs found.

```
from irfpy.ica.data_class import *
from irfpy.ica.modules import *

ICADataSet = ICAData(date, dataPath=dataPath, modeSel=msp//1e3, swSel=
    msp%1e3//10, paccSel=msp%10, cleanCT=False)

spec = np.nansum(ICADataSet.ionSpectraScan[:,:,:,e1:e2,m1:m2], axis=4)
      #nbScan x 16el x 16az x e2-e1

CT = np.nan_to_num(np.load('crosstalk.npy'))

for r in [0,1,2,3,4,6]:
  [k,l,m] = np.where(spec[:,:,r,:] != 0)
  spec[k,l,r,m] -= np.sum((CT[0,r,:]*np.log(spec[k,l,:,m].clip(1e-10))
     + CT[1,r,:])*spec[k,l,:,m].clip(1e-10), axis=1)
```

The quality of the data cleaning is presented with a few of the field-of-view comparison figures of the data sets that were not used in calculation of the cross-talk coefficients. These are data sets with the solar wind proton beam spread over more azimuth sectors.

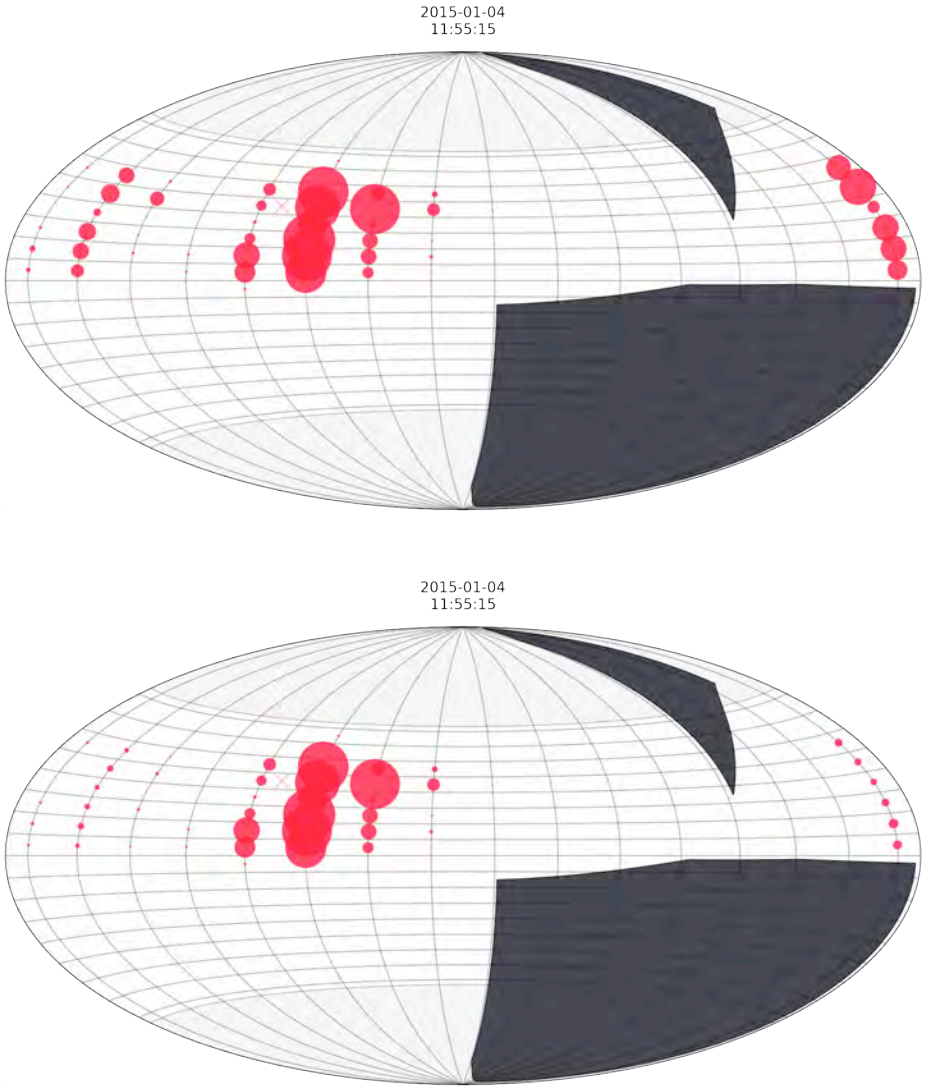

Figure 26: On the top original data set and on the bottom data set cleaned by applying the results of the empirical analysis. Negative values that may appear when subtracting the predicted value of cross-talk are presented as absolute values, to give a better idea about the quality of results.

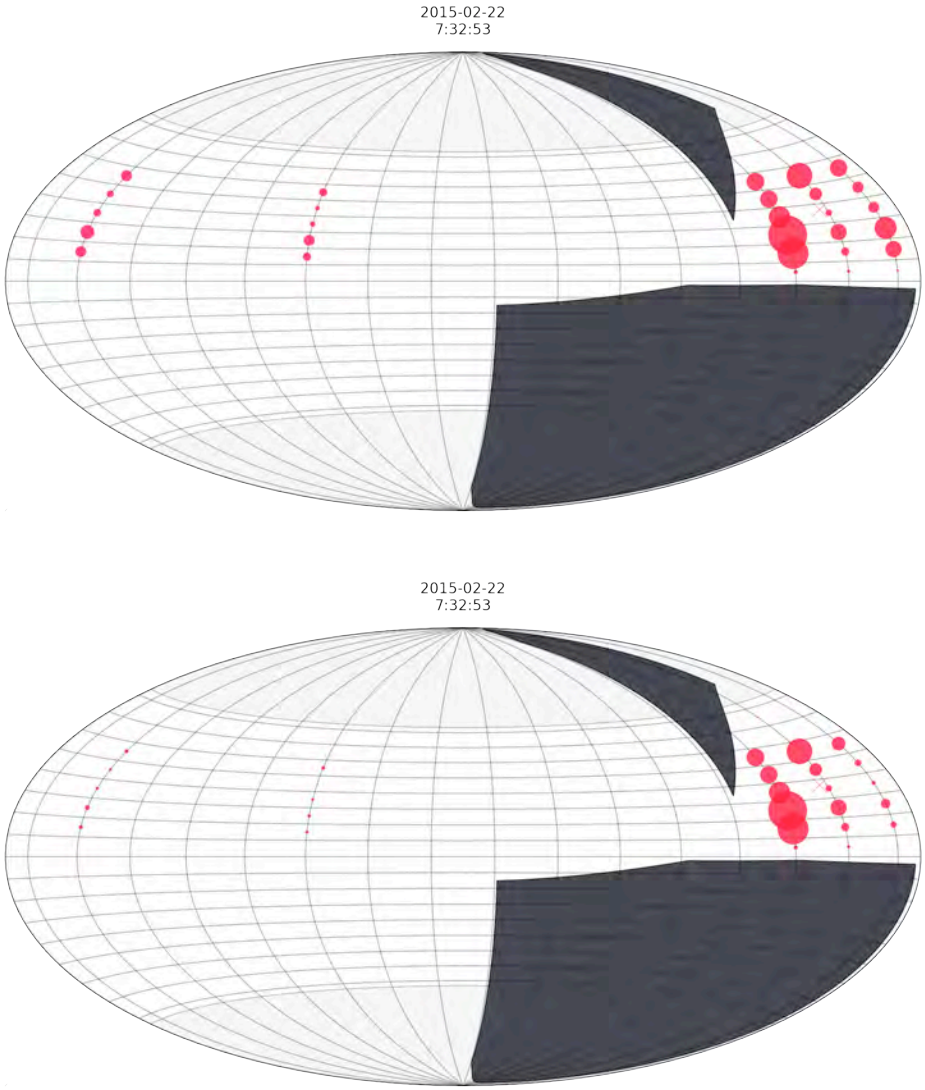

Figure 27

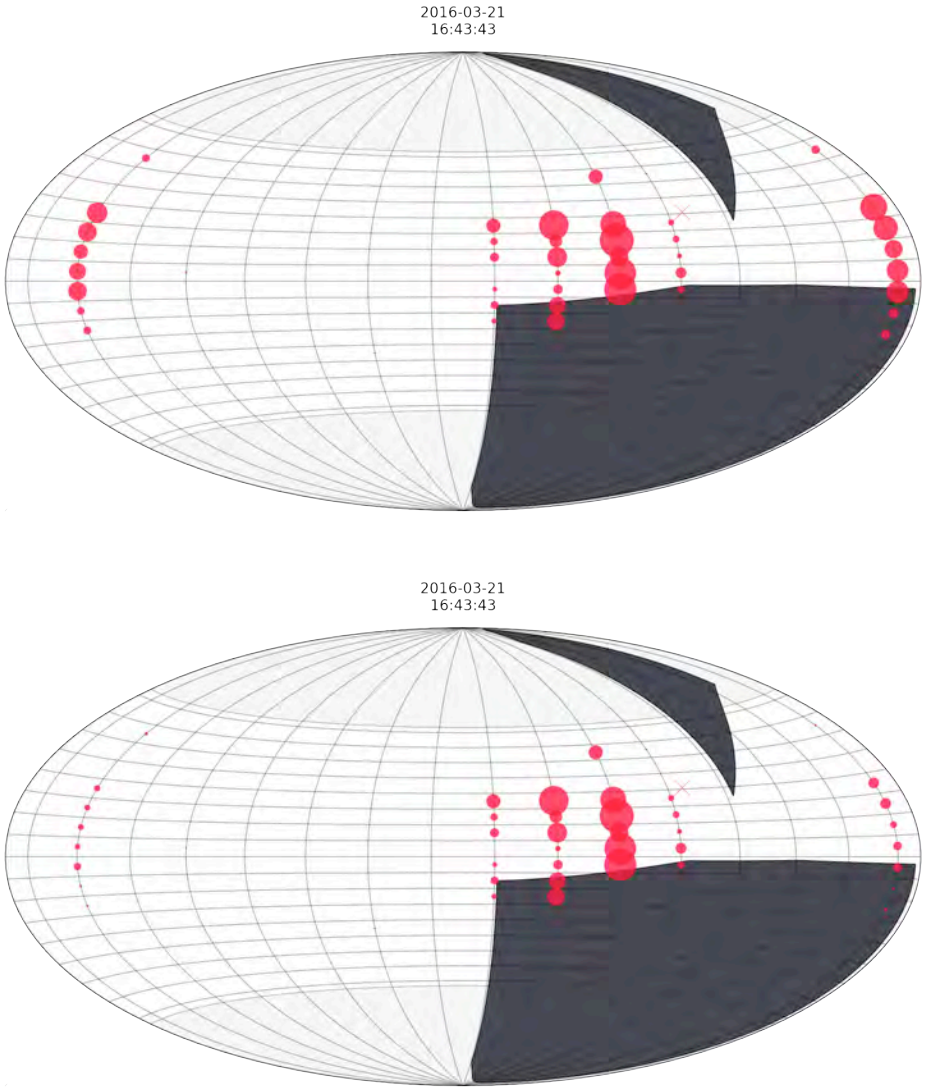

Figure 28

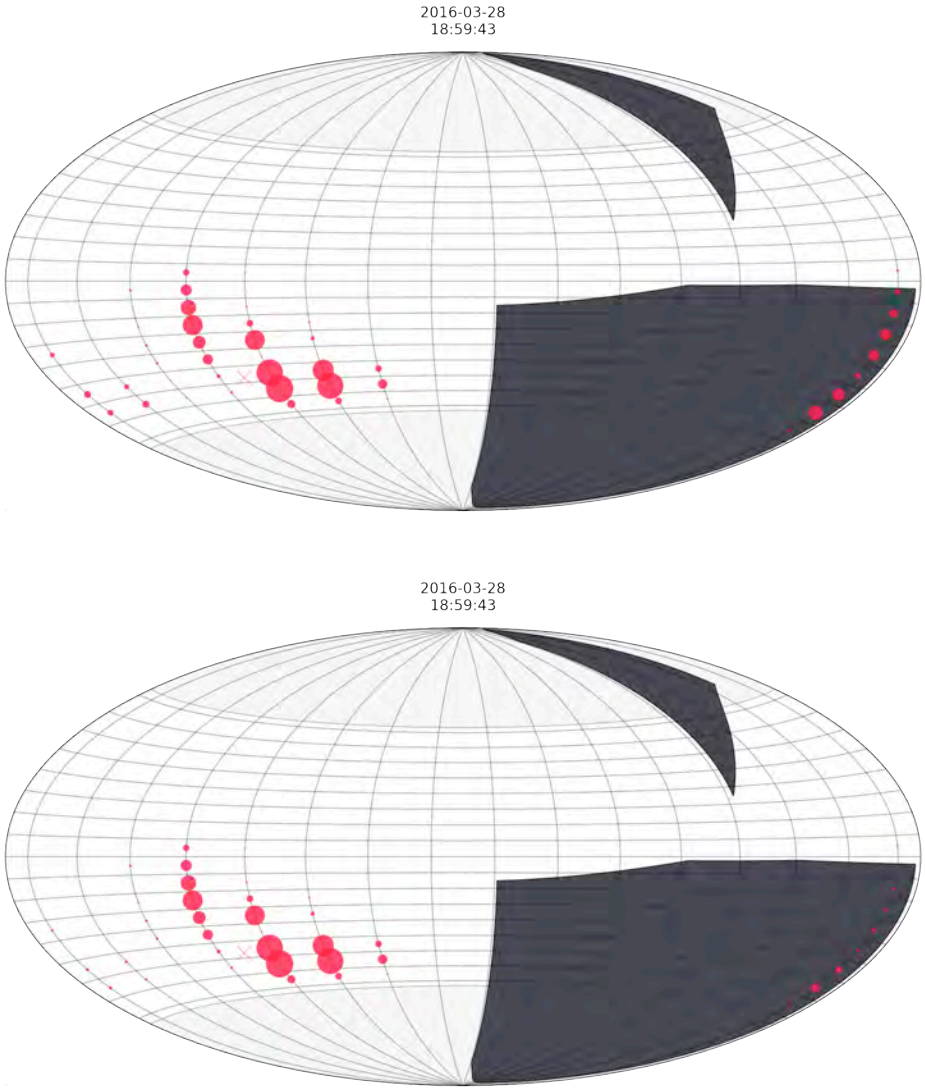

Figure 29

4 Theoretical Approach and documentation retrieval

4.1 Electronic Cross-Talk

Cross-talk is one of the noise sources in integrated circuits. The reason for its existence is the capacitive coupling between two wires that are situated either too closely together, or are not properly isolated, or both. In practice, a part of the signal from one of these two wires, will be transferred through the parasitic capacitor to the second one. Transmitted signal is stronger when capacitance is higher, that is when the wires are closer together. The parasitic capacitor may appear close to an amplifier, forming a bond between an already amplified signal and the second wire just in front of the amplifier. This will result in an even bigger cross-talk.

To determine the cross-talk with theoretical model of parasitic capacitance, one would need a detailed electronic structure report including information about the wires size, the distance between them, the position of amplifiers, and how they are wired to the MO-CADs.

Another potential source of cross-talk could be the signal processing logic that takes place after the signal reaches the FPGA. FPGA coding is not the same on ICA and IMA and we currently have no information about it.

4.2 ICA On-Ground Calibration Report

When ICA was calibrated by Andrei Fedorov in Toulouse, the following plot (Figure 30) was produced regarding the calibration of azimuth sectors and mass anode rings. The experiment was conducted by connecting one azimuth sector and running the proton beam horizontally over all 16 sectors. Its purpose was to see the response of the chosen sector to the ion beam position. Due to the ion beam instability, the horizontal patterns occur on the plots. Unfortunately, only plots of the experiment for sectors 0, 2, and 15 are still available and there is no information on the values of the colour map either. What can be concluded from these plots is that:

- sector 0 is affected by all other sectors,
- sector 2 is affected when ion beam illuminates sectors 6, 7, 10, 11, 14, and 15,
- sector 15 is affected when ion beam illuminates sectors 2, 3, and 4.

The colour maps that can be affiliated with the empirically obtained results, are the first two in the second row of Figure 30. These are the configurations that investigate the response of sector 0 and sector 2. The plots corroborate what was established by the data analysis: sectors 6, 7, 10, 11, 14 and 15 cause cross-talk in sector 2, and all sectors cause cross-talk in sector 0.

The third plot in the second row of Figure 30 does not contain much information since the bottom left corner, implying that sector 15 is receiving signal from sectors 2, 3 and 4, is active in all six plots and could be a consequence of noise during the experiment.

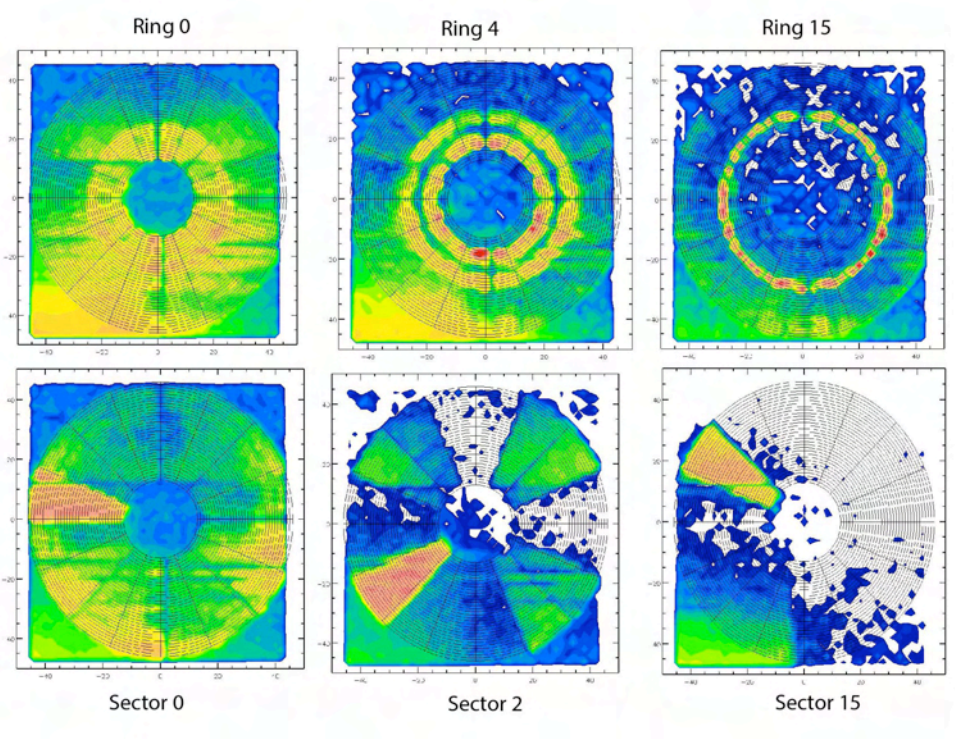

Figure 30: Selected Ring/Sector response to ion beam position: Top row shows the spatial distribution of count rate of selected rings and the bottom row of the selected sectors. [3]

4.3 IMA Documentation

Ion Mass Analyser (IMA) is a part of the the ASPERA-3 (Analyser of Space Plasma and Energetic Atoms) instrument of Mars Express, designed to study the solar wind interaction with the Mars atmosphere and to characterise the plasma and neutral gas environment near Mars. The pre-amplifying board for ICA is the engineering unit for IMA, leading everyone involved in its manufacture (that were still reachable) to believe that the electronic structure of ICA and IMA is identical. The proof of that are the pictures of both boards, presented in Figure 32 and 31. The boards were designed at IRF Kiruna, but later passed on to the South West Research Institute (San Antonio, Texas).

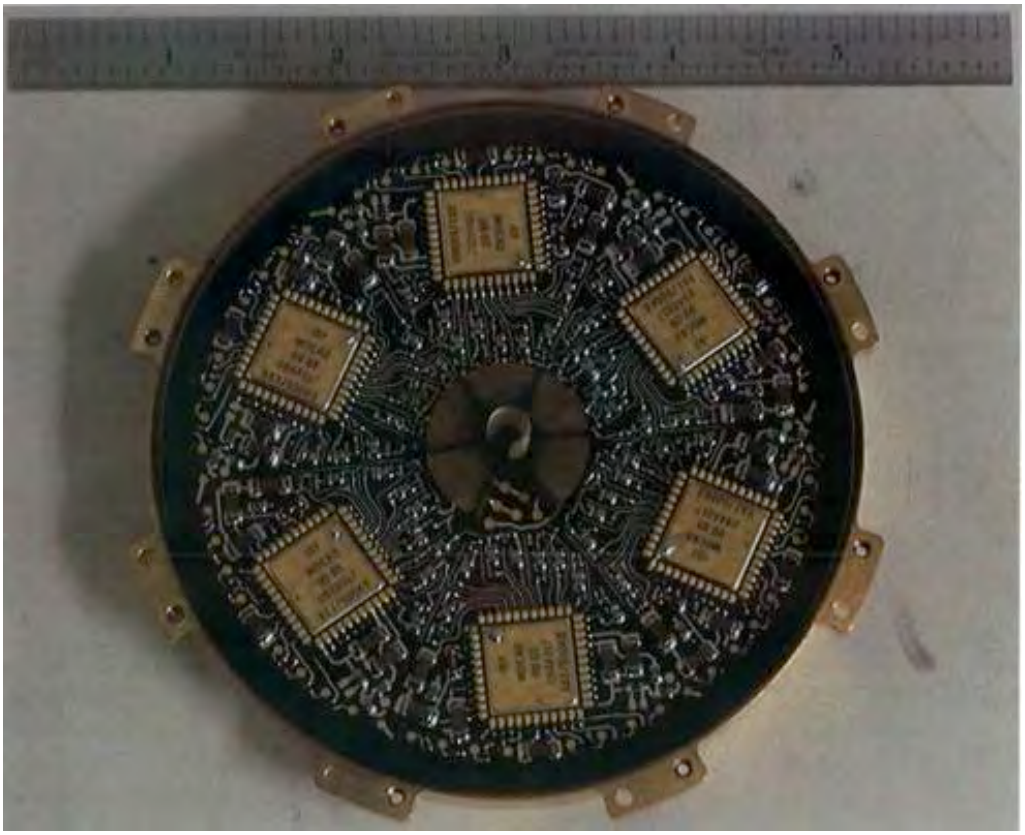

Figure 31: IMA - electronic board.

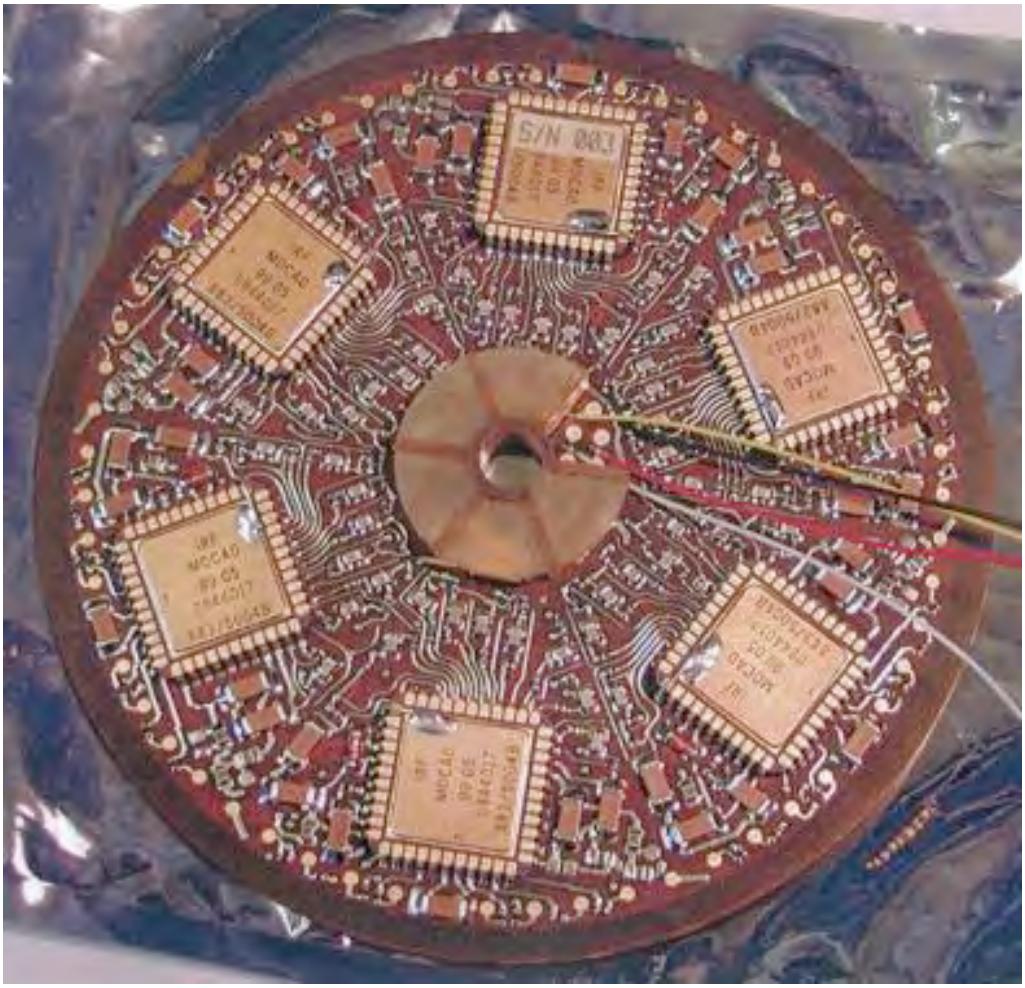

Figure 32: ICA - electronic board.

This is a great advantage, allowing us to use IMA documentation to investigate cross-talk between the azimuth sector anodes of ICA. The on-ground calibration for IMA, same as for ICA, was made in Toulouse and the retrieved document includes the colour map plots of the cross-talk for selected mass anode rings and sectors (Figure 33). Conclusions from the three plots in the second row, presenting azimuth sector response, are:

- sector 1 is affected when ion beam illuminates sectors 3, 5 and 9,
- sector 5 is not affected by any other sector,
- sector 6 is affected when ion beam illuminates sectors 14 and 15.

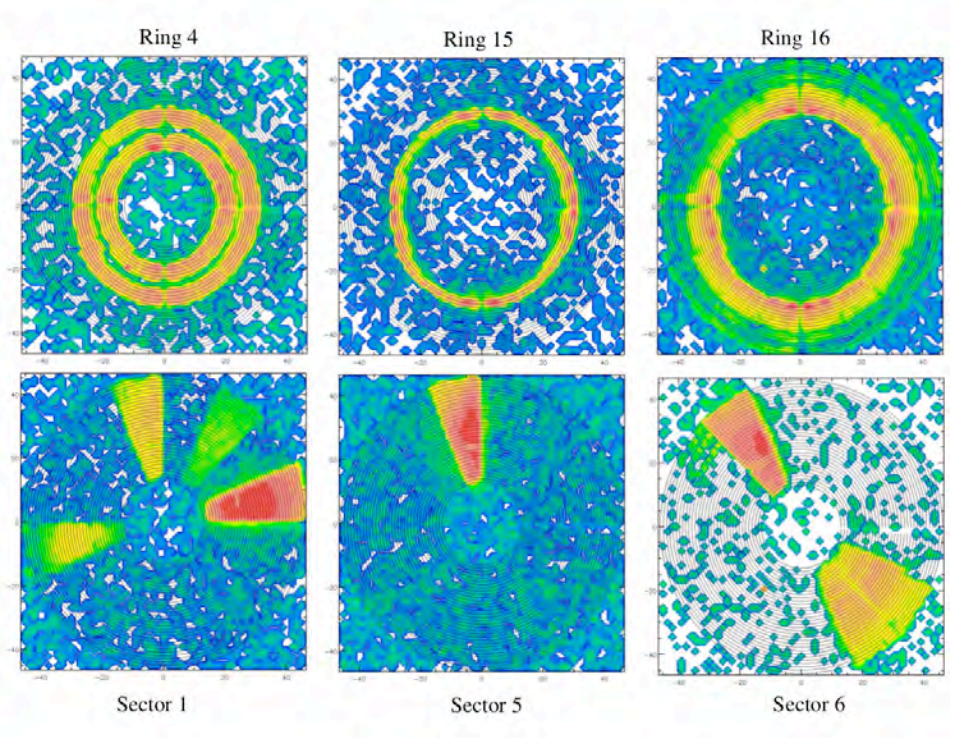

Figure 33: Selected Ring/Sector response to ion beam position: Top row shows the spatial distribution of count rate of selected rings and the bottom row of the selected sectors. Note that azimuth sectors are rotated 180^o clockwise. [4]

The first and the third plot in the second row of Figure 33, showing the response of sector 1 and sector 6 can be related to in-flight calibration results. Data analysis has confirmed the correlation between sectors 5 and 1, and 9 and 1, but not the weak correlation between sector 3 and 1. Also sector 6 has been proved to be a receiver for sectors 14 and 15.

Furthermore, the middle plot contains a significant information: there is no cross-talk in sector 5.

Table 4: Cross-talking pairs that appear in the on-ground calibration reports for ICA and IMA.

Emitter	Reciever
3	1
5	1
6	2
7	2
9	1
10	2
11	2
14	2 6
15	2 6
all	0
none	5

Electronic structure

It is not possible to get the electronic structure report for ICA, but we were able to retrieve the electronics schematics for IMA. It includes the internal trace of the ring layer, showing how mass anode rings and azimuth sectors are connected to the six MOCADs (Figure 34).

The schematics (Figure 34) implies that the good candidates for cross-talking pairs (sector pairs that are connected to the same MOCAD very close to each other) are sectors: 0 and 1, 2 and 3, 6 and 7, 8 and 9, 10 and 11, and 14 and 15. None of this pairs have been found as cross-talking by empirical approach, because the analysis was limited to azimuth sectors situated at least one sector apart from each other. The neighbouring sectors in some cases do show similar properties, like sectors 6 and 7 both emitting to sector 2, and the same goes for sectors 10 and 11, and 14 and 15.

However, there appears to be another mechanism causing electronic cross-talk between sectors situated 90^o or more apart.

5 Further research

Empirical Research

During my research I have made a list of special data sets that might be further analysed and maybe reveal more about the cross-talk phenomena.

Next step would be applying the resulting cross-talk matrix to the full data base and check if a larger time period could be considered, based on the solar wind characteristics along the mission, an overview of which (including velocity distributions) is given in the submitted paper [5].

Another direction would be to study the scientific data from IMA instrument and check whether it shows the same properties of cross-talk, since it has the same amplifying

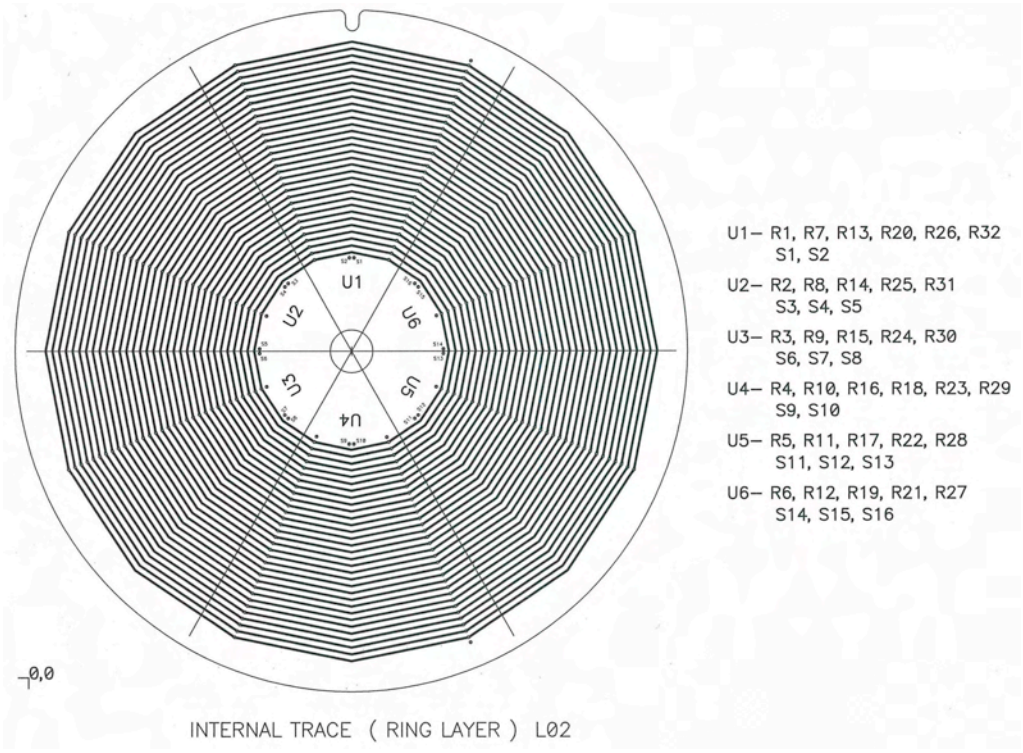

Figure 34: $U1$ - $U6$ represent the six MOCADs used on the IMAs amplifier board. $R1$ - $R32$ are the 32 mass anode rings and $S1$ - $S16$ the 16 azimuth sectors. (Note: Numbering of sectors in this scheme starts with 1, not with 0 as in previous discussion.)

board as ICA.

Theoretical Research

For a better understanding of cross-talk wonder in this instrument one would have to do further documentation archaeology, in order to find detailed information about the instrument's electronic structure and FPGA coding.

In the report it was found that cross-talk is dependant on the number of protons detected. It would be interesting to try to model the circumstances that would produce the logarithmic trend that has been observed with data analysis. One already proposed explanation is the one- or two-count reduction operated on-board the spacecraft, and its effect on small signals.

6 Conclusion

The empirical approach to the problem of the cross-talk between azimuth sectors on Ion Composition Analyzer proved out to be successful. Due to the uniformity of the solar wind proton beam during a long period of the mission, we were able to accurately

determine cross-talk properties for most of the azimuth sectors. The cross-talk pairs obtained by data analysis agree with the plots from the on-ground calibration report of ICA and IMA. The validated retrieved documentation has provided us with the potential cross-talking sector pairs that are still to be examined with different statistical analysis approaches also including heavier ions.

The two complementing approaches gave reliable results that tackle one of the most crippling aspect of this fresh data base. Further more, these findings might be applicable to the Ion Mass Analyzer, the instrument with identical amplifying board to ICA, but a part of the Mars Express mission.

Table 5: The resulting 16 times 16 sector matrix showing the cross-talk percentage averaged for $N_{emitter} = 1000$. Lines represent receivers and columns emitters.

	0	1	2	3	4	5	6	7	8	9	10	11	12	13	14	15
0	0		33.7	31.8	31.5	18.3	19.9	30.2	36.2	29.8	31.1	25.9	43.7		21.8	
1	0	0	0	0	0	8.4	0	0	0	2.5	0	0	0	0	0	0
2	0	0	0	0	0	0	10.3	4.5	0	0	25.8	28.1	0	0	11.9	19.1
3				0		0	0	8.7	0	0	0	0	0		0	0
4					0	0	0	0	0	0	0	0	7.1		0	0
5	0	0	0	0	0	0	0	0	0	0	0	0	0	0	0	0
6	0	0	0	0	0	0	0	0	0	0	0	0	0	0	8.1	7.8
7					0	0	0	0	0	0	0	0	0		0	0
8					0	0	0	0	0	0	0	0	0		0	0
9					0	0	0	0	0	0	0	0	0		0	0
10					0	0	0	0	0	0	0	0	0		0	0
11					0	0	0	0	0	0	0	0	0		0	0
12					0	0	0	0	0	0	0	0	0		0	0
13					0	0	0	0	0	0	0	0	0	0	0	0
14					0	0	0	0	0	0	0	0	0		0	
15	0	0	0	0	0	0	0	0	0	0	0	0	0	0	0	0

References

[1] H.Nilsson: *RPC-ICA: The Ion Composition Analyzer of the Rosetta Plasma Consortium*, 2007

[2] *SCHEMATIC, ION MASS ANALYZER*, Southwest Research Institute, San Antonio, Texas

[3] Andrei Fedorov: *ICA (ROSETTA) calibration report*, CESR-CNRS, Toulouse, France

[4] Andrei Fedorov: *IMA calibration report*, CESR-CNRS, Toulouse, France

[5] Behar et al: *The birth and growth of a solar wind cavity around a comet - Rosetta observations*, MNRAS 2017 (submitted)

7 Appendix

1. Cross-talk plots for sector 0
2. The CT matrix 'crosstalk.npy'z

Appendix 1 - Cross-talk plots for sector 0

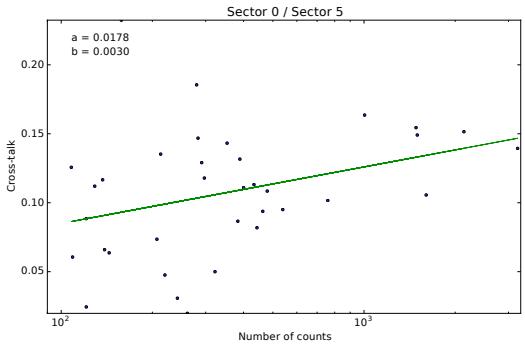

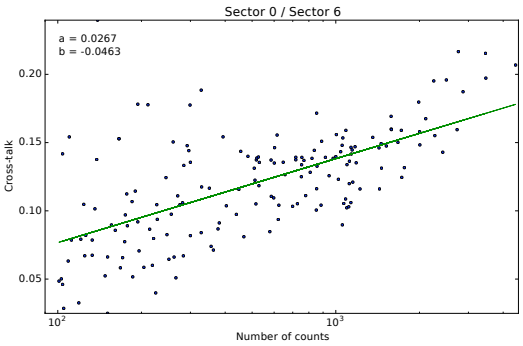

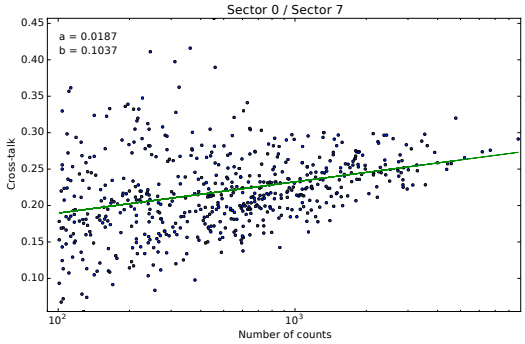

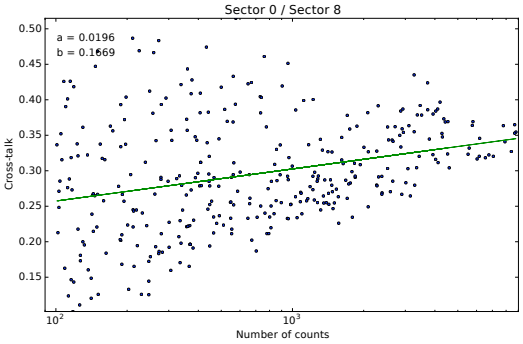

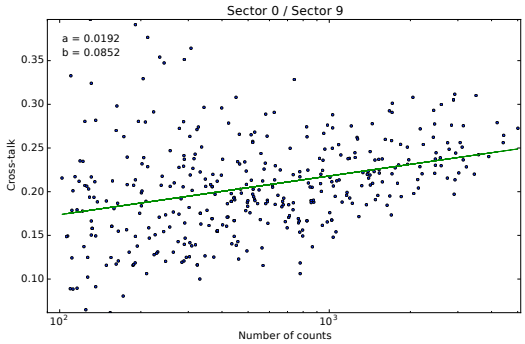

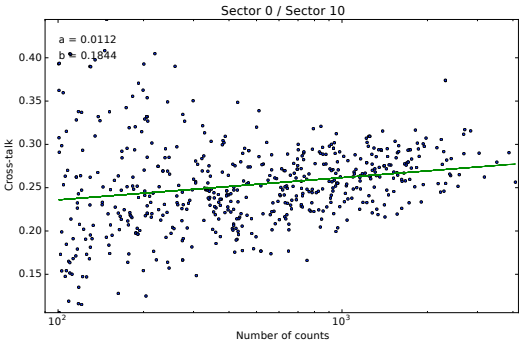

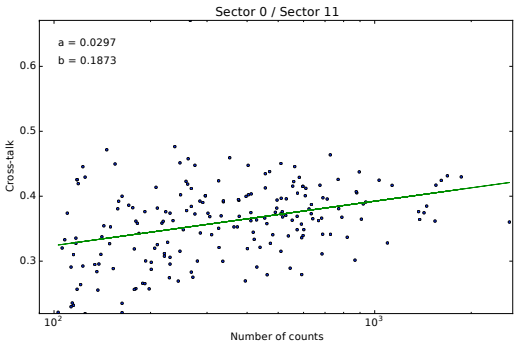
Sector 0 / Sector 11
a = 0.0297
b = 0.1873
Cross-talk
0.6
0.5
0.4
0.3
10^2
10^3
Number of counts

Appendix 2 - The CT matrix: ’crosstalk.npy’

a	0	1	2	3	4	5	6	7	8	9	10	11	12	13	14	15
0	0	nan	0.015	0.014	0.012	0.020	0.012	0.032	0.036	0.030	0.026	-0.005	0.003	nan	0	nan
1	0	0	0	0	0	0.015	0	0	0	0.003	0	0	0	0	0	0
2	0	0	0	0	0	0	0.014	0.005	0	0	0.021	0.015	0	0	0.014	0.018
3	nan	nan	nan	0	nan	0	0	0.012	0	0	0	0	0	nan	0	0
4	nan	nan	nan	nan	0	nan	0	0	0	0	0	0	0.011	nan	0	0
5	0	0	0	0	0	0	0	0	0	0	0	0	0	0	0	0
6	0	0	0	0	0	0	0	0	0	0	0	0	0	0	0.014	0.012
7	nan	nan	nan	nan	0	0	0	0	0	0	0	0	0	nan	0	0
8	nan	nan	nan	nan	0	0	0	0	0	0	0	0	0	nan	0	0
9	nan	nan	0	0	0	0	0	0	0	0	0	0	0	nan	0	0
10	nan	nan	0	0	0	0	0	0	0	0	0	0	0	nan	0	0
11	nan	nan	0	0	0	0	0	0	0	0	0	0	0	nan	0	0
12	nan	nan	0	0	0	0	0	0	0	0	0	0	0	nan	0	0
13	nan	nan	0	0	0	0	0	0	0	0	0	0	0	0	0	0
14	nan	nan	0	0	0	0	0	0	0	0	0	0	0	nan	0	0
15	0	0	0	0	0	0	0	0	0	0	0	0	0	nan	0	0

b	0	1	2	3	4	5	6	7	8	9	10	11	12	13	14	15
0	0	nan	0.236	0.218	0.231	0.047	0.119	0.084	0.117	0.094	0.133	0.291	0.413	nan	0.221	nan
1	0	0	0	0	0	-0.022	0	0	0	0.004	0	0	0	0	0	0
2	0	0	0	0	0	0	0.007	0.010	0	0	0.113	0.180	0	0	0.025	0.066
3	nan	nan	nan	0	nan	0	0	0.006	0	0	0	0	0	nan	0	0
4	nan	nan	nan	nan	0	nan	0	0	0	0	0	0	-0.007	nan	0	0
5	0	0	0	0	0	0	0	0	0	0	0	0	0	0	0	0
6	0	0	0	0	0	0	0	0	0	0	0	0	0	0	-0.014	-0.008
7	nan	nan	nan	nan	0	0	0	0	0	0	0	0	0	nan	0	0
8	nan	nan	nan	nan	0	0	0	0	0	0	0	0	0	nan	0	0
9	nan	nan	0	0	0	0	0	0	0	0	0	0	0	nan	0	0
10	nan	nan	0	0	0	0	0	0	0	0	0	0	0	nan	0	0
11	nan	nan	0	0	0	0	0	0	0	0	0	0	0	nan	0	0
12	nan	nan	0	0	0	0	0	0	0	0	0	0	0	nan	0	0
13	nan	nan	0	0	0	0	0	0	0	0	0	0	0	0	0	0
14	nan	nan	0	0	0	0	0	0	0	0	0	0	0	nan	0	0
15	0	0	0	0	0	0	0	0	0	0	0	0	0	nan	0	0

INSTITUTET FÖR RYMDFYSIK

Swedish Institute of Space Physics

Swedish Institute of Space Physics
Box 812, SE- 981 28 Kiruna, SWEDEN
tel. +46-980-790 00, fax +46-980-790 50, e-post: irf@irf.se

www.irf.se